


RESEARCH ARTICLE

Open Access



Mutant *C. elegans* mitofusin leads to selective removal of mtDNA heteroplasmic deletions across generations to maintain fitness

Lana Meshnik¹, Dan Bar-Yaacov^{1,2}, Dana Kasztan¹, Tali Neiger¹, Tal Cohen¹, Mor Kishner¹, Itay Valenci¹, Sara Dadon¹, Christopher J. Klein³, Jeffery M. Vance⁴, Yoram Nevo⁵, Stephan Züchner⁴, Ofer Ovadia¹, Dan Mishmar¹ and Anat Ben-Zvi^{1*} 

Abstract

Background: Mitochondrial DNA (mtDNA) is present at high copy numbers in animal cells, and though characterized by a single haplotype in each individual due to maternal germline inheritance, deleterious mutations and intact mtDNA molecules frequently co-exist (heteroplasmy). A number of factors, such as replicative segregation, mitochondrial bottlenecks, and selection, may modulate the existence of heteroplasmic mutations. Since such mutations may have pathological consequences, they likely survive and are inherited due to functional complementation via the intracellular mitochondrial network. Here, we hypothesized that compromised mitochondrial fusion would hamper such complementation, thereby affecting heteroplasmy inheritance.

Results: We assessed heteroplasmy levels in three *Caenorhabditis elegans* strains carrying different heteroplasmic mtDNA deletions (Δ mtDNA) in the background of mutant mitofusin (*fzo-1*). Animals displayed severe embryonic lethality and developmental delay. Strikingly, observed phenotypes were relieved during subsequent generations in association with complete loss of Δ mtDNA molecules. Moreover, deletion loss rates were negatively correlated with the size of mtDNA deletions, suggesting that mitochondrial fusion is essential and sensitive to the nature of the heteroplasmic mtDNA mutations. Introducing the Δ mtDNA into a *fzo-1;pdr-1*; $+/ \Delta$ mtDNA (PARKIN ortholog) double mutant resulted in a skewed Mendelian progeny distribution, in contrast to the normal distribution in the *fzo-1*; $+/ \Delta$ mtDNA mutant, and severely reduced brood size. Notably, the Δ mtDNA was lost across generations in association with improved phenotypes.

Conclusions: Taken together, our findings show that when mitochondrial fusion is compromised, deleterious heteroplasmic mutations cannot evade natural selection while inherited through generations. Moreover, our findings underline the importance of cross-talk between mitochondrial fusion and mitophagy in modulating the inheritance of mtDNA heteroplasmy.

Keywords: *C. elegans*, *fzo-1*, Heteroplasmy inheritance, Mitofusin, mtDNA, PARKIN, *pdr-1*

Background

Unlike the nuclear genome, mitochondrial DNA (mtDNA) is present in multiple copies per animal cell. For instance, each human somatic cell contains an average of ~1000 mitochondria, with each mitochondrion harboring 1–10 mtDNA copies [1]. Although

*Correspondence: anatbz@bgu.ac.il

¹ Department of Life Sciences, Ben-Gurion University of the Negev, Beer Sheva, Israel

Full list of author information is available at the end of the article



© The Author(s) 2022. **Open Access** This article is licensed under a Creative Commons Attribution 4.0 International License, which permits use, sharing, adaptation, distribution and reproduction in any medium or format, as long as you give appropriate credit to the original author(s) and the source, provide a link to the Creative Commons licence, and indicate if changes were made. The images or other third party material in this article are included in the article's Creative Commons licence, unless indicated otherwise in a credit line to the material. If material is not included in the article's Creative Commons licence and your intended use is not permitted by statutory regulation or exceeds the permitted use, you will need to obtain permission directly from the copyright holder. To view a copy of this licence, visit <http://creativecommons.org/licenses/by/4.0/>. The Creative Commons Public Domain Dedication waiver (<http://creativecommons.org/publicdomain/zero/1.0/>) applies to the data made available in this article, unless otherwise stated in a credit line to the data.

this intracellular mtDNA population is inherited from the maternal germline and hence carries a single major haplotype, mtDNA molecules can differ in sequence (heteroplasmy) either due to inheritance of mutations from the ovum or due to the accumulation of changes over an individual lifetime [2–5]. Some of these changes may have pathological consequences [6, 7], as reflected in a variety of mitochondrial disorders, yet only upon crossing a threshold of prevalence in the cell [8]. Accordingly, the penetrance of disease-causing mutations ranges between 60 and 80%, depending on the symptoms and tissues that display the specific phenotype [9].

The repertoire of heteroplasmic mutations varies among cells and tissues, mainly due to replicative segregation (drift) of the mitochondria during cell division and mitochondrial bottlenecks that appear during embryo development [10]. However, it has been suggested that heteroplasmy can be modulated by non-random factors, including selection [2, 4, 5, 11, 12]. Indeed, it has been shown that mitophagy, a mechanism of mitochondrial quality control, partially provides selection against defective mitochondria and maintains disease-causing mtDNAs below the threshold levels both in human cells [13] and in a *Caenorhabditis elegans* model system [14–17]. Mitophagy requires proper fission-fusion cycles of the mitochondrial network to allow the removal of dysfunctional mitochondria [18, 19]. In agreement with this notion, elevated heteroplasmy levels of pathological mtDNA molecules were observed when the fission machinery was disrupted in cell culture [20]. Furthermore, reduction in heteroplasmy levels of potentially deleterious mtDNA mutations was observed when components of the fusion machinery were compromised in *Drosophila* model systems, especially in germ cells [12, 21, 22]. In consistence with this notion, cell culture experiments revealed that a mixture of mtDNA molecules differing in sequence in the same cell can complement each other by the diffusion of products via the mitochondrial network, which in turn leads to restoration of mitochondrial function [1, 15, 16, 23]. Hence, mitochondrial fusion likely allows the survival of mtDNA disease-causing mutations in cells and, in turn, their transmission to the next generation [1, 8, 24]. Although these experiments suggest a molecular mechanism for the control of heteroplasmy, it remains unclear whether such a mechanism also affects the transmission of heteroplasmy through generations. Investigating this problem will allow explaining the relatively high abundance of low-level disease-causing heteroplasmic mutations in the general population [25, 26]. We, therefore, hypothesized that interfering with the intracellular mitochondrial network by compromising the fusion machinery would

hamper mitochondrial functional complementation and thus impede the inheritance of heteroplasmic mutants.

Here, we took the first steps towards testing this hypothesis by crossing *C. elegans* harboring mitofusin mutant (*fzo-1*) to animals carrying either of three heteroplasmic mtDNA deletions, which differed in size and mtDNA positions. These experiments resulted in embryonic lethality and developmental delay, which were alleviated in subsequent generations concomitant with a complete loss of the truncated mtDNA molecules. Since the rate of truncated mtDNA loss diverged between the heteroplasmic strains, the sensitivity of the fusion machinery to different mtDNA mutations, in addition to its interaction with mitophagy and relevance to human diseases are discussed.

Results

A heteroplasmic deletion reduces the fitness of *C. elegans* mitofusin (*fzo-1*) mutant

The stable heteroplasmic *C. elegans* strain *uaDf5/+* harbors a mixture of intact (+mtDNA) and ~ 60% of a 3.1 kb mtDNA deletion (Δ mtDNA) [27]. Although lacking four essential genes (i.e., mt-ND1, mt-ATP6, mt-ND2, and mt-Cytb) and seven tRNAs (i.e., K, L, S, R, I, Q and F), this strain is viable and displays some mitochondrial dysfunction [16, 27, 28]. High heteroplasmy levels are likely not maintained due to mtDNA duplication but by stably maintaining +mtDNA copy number [16]. We showed that dysfunctional PDR-1, the worm orthologue of the key mitophagy factor Parkin (PARK2), led to elevated levels of the truncated mtDNA, suggesting that mitochondrial quality control can modulate the levels of dysfunctional mitochondria [14]. In conjunction with this finding, RNAi knockdown of *fzo-1*, the *C. elegans* orthologue of MFN1/2, led to a slight reduction in the levels of the heteroplasmic Δ mtDNA, although without any phenotypic consequences [15]. We, therefore, asked what would be the impact of the *fzo-1(tm1133)* deletion (hereafter designated as *fzo-1(mut)*) on the inheritance of the Δ mtDNA.

To this end, we crossed *uaDf5/+* heteroplasmic hermaphrodites (+/ Δ mtDNA) with *fzo-1(mut)* heterozygote males (Fig. 1A). After self-cross of the F1 progeny, the distribution of the genotypes in the F2 heteroplasmic progeny did not deviate from the expected Mendelian ratio, namely 26% homozygous *fzo-1(mut)*, 48.7% *fzo-1* heterozygotes (*ht*), and 25.3% *fzo-1* wild type (*wt*) (chi-square test, $P = 0.960$; Additional file 1: Table S1). However, we noticed that only $13 \pm 5\%$ of the progeny of the self-crossed *fzo-1(mut);+/ Δ mtDNA* worms hatched, as compared to *fzo-1(mut)* animals ($67 \pm 5\%$, ANOVA followed by a Tukey's post hoc test, $P < 0.001$; Fig. 1B). Although mitochondrial organization and TMRE uptake

of self-crossed *fzo-1(mut);+/ Δ mtDNA* adults were similar to *fzo-1(mut)* (Additional file 1: Fig. S1A-B), *fzo-1(mut);+/ Δ mtDNA* animals were developmentally delayed, and none of them reached adulthood after six days as compared to *fzo-1(mut)* (ANOVA followed by a Tukey's post hoc test, $P < 0.001$). This was in contrast to self-crossed *fzo-1(wt);+/ Δ mtDNA* animals, all of which reached adulthood after six days (Fig. 1C). These findings demonstrate that the interaction between the heteroplasmic Δ mtDNA and the nuclear DNA-encoded *fzo-1* mutant led to a severe reduction in fitness.

The adverse effects of the interaction between Δ mtDNA and *fzo-1(mut)* are reversed across generations

To better characterize the phenotypic impact of the interactions between Δ mtDNA and *fzo-1(mut)*, we monitored the development of progeny of the self-crossed *fzo-1(ht);+/ Δ mtDNA* worms, followed by genotyping the resultant adult animals (generation 1, G1). We continued to follow the hatching and development of their progeny, i.e., *fzo-1(mut);+/ Δ mtDNA* (G2m) and *fzo-1(wt);+/ Δ mtDNA* (G2wt), across four generations (Fig. 2A). Specifically, we measured the duration of the larva-to-adulthood period during development in the G1m-G4m generations (Fig. 2B). While ~75% of the G1m animals reached adulthood after 6 days, the development of G2m animals was 1.9-fold delayed (Cox proportional-hazards regression, $P < 0.001$), with 75% of the animals reaching adulthood only after 9 days. Surprisingly, the G3m animals showed significant improvement (Cox proportional-hazards regression, $P < 0.001$), with ~60% of this population reaching adulthood after six days. Moreover, G4m animals showed a full reversal of Δ mtDNA-associated adverse effects (Cox proportional-hazards regression, $P = 0.750$; Fig. 2B and Additional file 1: Table S2). We noted a similar pattern across generations when hatching was considered: In contrast to the 13.5% hatching observed among G2m embryos, 60 \pm 8% hatching of the G3m embryos was observed (ANOVA followed by a Tukey's post hoc test, $P < 0.001$). The hatching percentage of the G4m generation was similar

to that of G1 animals (71 \pm 9% and 67 \pm 5%, respectively, ANOVA followed by a Tukey's post hoc test $P = 0.993$) and remained stable over subsequent generations (Fig. 2C). Finally, no phenotypic changes were observed for G1wt-G4wt animals while tracing their developmental pace (Cox proportional-hazards regression, $P > 0.140$; Additional file 1: Table S2) and hatching percentage (ANOVA followed by a Tukey's post hoc test, $P > 0.266$; Additional file 1: Fig. S2A-B). Taken together, our findings demonstrate a full reversal of the adverse effects of the interaction between the Δ mtDNA and the nuclear DNA-encoded mutant *fzo-1* gene.

fzo-1(mut) leads to selection against Δ mtDNA heteroplasmy in *C. elegans*

We next asked how the deleterious interactions between *fzo-1(mut)* and Δ mtDNA were abrogated. We hypothesized that if the Δ mtDNA is not tolerated in the background of *fzo-1(mut)*, then selection against the Δ mtDNA should occur. To test this prediction, we assessed the levels of Δ mtDNA by quantitative PCR (qPCR, see Methods) across the G1m-G4m generations (using gravid adults) in both the *fzo-1(mut);+/ Δ mtDNA* and the *fzo-1(wt);+/ Δ mtDNA* strains. We found that Δ mtDNA levels declined by 10-fold in the G2m *fzo-1(mut)* animals, as compared to $+/ Δ mtDNA parental strain (Fractional regression, odds ratio = 0.08; $P < 0.001$). Values of Δ mtDNA reached below detection levels in most G3m ($N = 18/21$) and G4m ($N = 20/21$) animals (fractional regression, odds ratio < 0.007 , $P < 0.001$; Fig. 2D and Additional file 1: Table S3), while the relative levels of intact $+mtDNA$ molecules increased (Additional file 1: Fig. S2C and Table S3). In contrast, Δ mtDNA and $+mtDNA$ levels did not significantly change across the G1wt-G4wt generations of *fzo-1(wt);+/ Δ mtDNA* animals (fractional regression, $P = 0.852$; Fig. 2E and Additional file 1: S2D and Table S3).$

These results suggest that the Δ mtDNA was completely lost during the G1m-G4m generations. To test this hypothesis, we crossed G4m hermaphrodites with wild type males to isolate *fzo-1(wt)* progeny (Gm \rightarrow Gwt).

(See figure on next page.)

Fig. 1 Δ mtDNA reduces the fitness of *fzo-1(mut)* animals. **A** Establishing *fzo-1* mutant and wild type heteroplasmic lines. Heteroplasmic hermaphrodites carrying intact and truncated mtDNA [*uaDf5/+*] were crossed with *fzo-1(tm1133)* heterozygotes males, *fzo-1(ht)*. Cross progeny F1 were allowed to self-propagate. Single F2 animals were isolated, allowed to lay eggs, and their genotypes were determined using a single worm PCR. Heteroplasmic ($+/ Δ mtDNA$) mutant (*mut*) or wild type (*wt*) *fzo-1* progeny were then monitored. **B** The percent of hatched embryos of parental strains: N2 (WT; $N = 13$, $n = 869$), $+/ Δ mtDNA$ ($N = 7$, $n = 265$) and *fzo-1(mut)* ($N = 13$, $n = 386$), of *fzo-1(ht);+/ Δ mtDNA* animals ($N = 5$, $n = 152$) and of mutant, *fzo-1(mut);+/ Δ mtDNA* ($N = 7$, $n = 236$) or wild type *fzo-1(wt);+/ Δ mtDNA* ($N = 4$, $n = 104$) cross progeny. Data are means \pm 1 standard error of the mean (1SE). Data were analyzed using one-way ANOVA followed by a Tukey's post hoc test. (*) denotes $P < 0.05$ and (**) denotes $P < 0.001$ compared with WT animals. **C** The percent of gravid adults six days after egg laying of parental strains: N2 (WT) ($N = 5$, $n = 114$), $+/ Δ mtDNA$ ($N = 9$, $n = 232$) and *fzo-1(mut)* ($N = 4$, $n = 278$), of *fzo-1(ht);+/ Δ mtDNA* animals ($N = 5$, $n = 69$), and of mutant, *fzo-1(mut);+/ Δ mtDNA* ($N = 4$, $n = 152$) or wild type *fzo-1(wt);+/ Δ mtDNA* ($N = 5$, $n = 245$) cross progeny. Data are means \pm 1 standard error of the mean (1SE). Data were analyzed using one-way ANOVA followed by a Tukey's post hoc test. (**) denotes $P < 0.001$ compared with WT animals. Individual data values are presented in Additional file 2

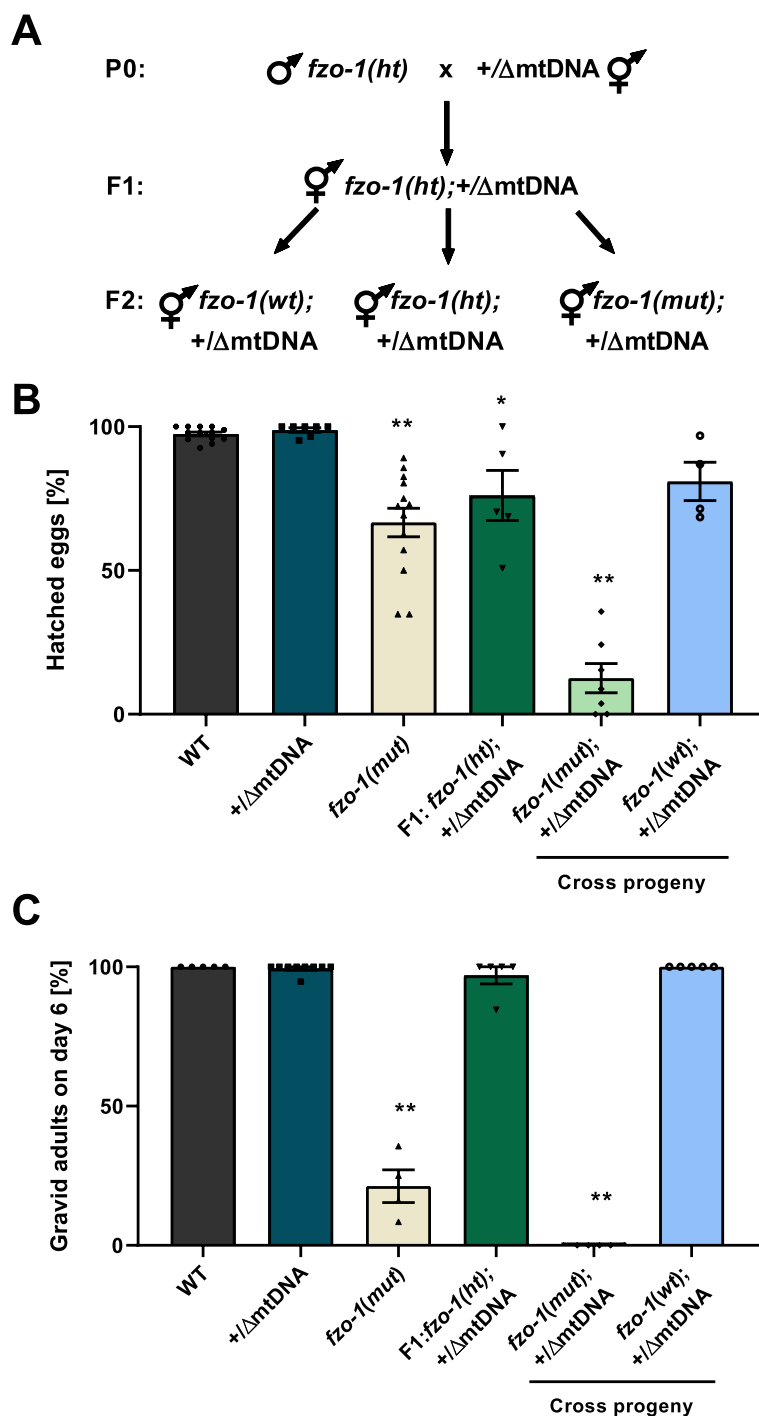


Fig. 1 (See legend on previous page.)

Since traces of Δ mtDNA were neither detected in Gm->Gwt animals (fractional regression, $P < 0.001$; Fig. 2D) nor in subsequent generations (ANOVA followed by a Tukey’s post hoc test, $P < 0.001$; Fig. 2F), we concluded that disrupting *fzo-1* function indeed resulted in a

complete and specific loss of the deleterious heteroplasmic Δ mtDNA. These results provide a proof of concept that mitochondrial fusion is critical for regulating the transmission of the *uaDf5* Δ mtDNA heteroplasmy across generations.

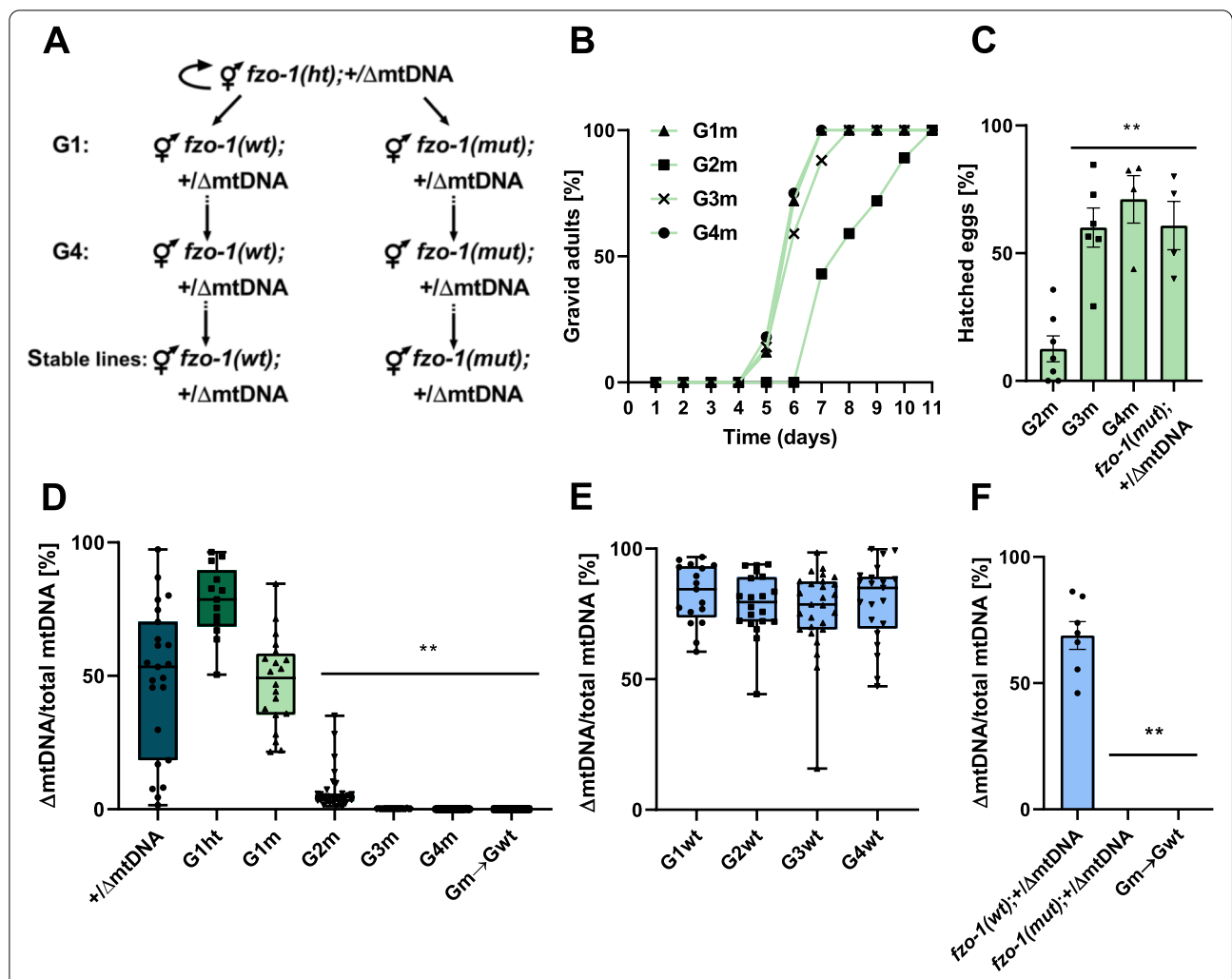


Fig. 2 Δ mtDNA levels are selectively eliminated, and their adverse effects reversed in *fzo-1(mut);+/\Delta*mtDNA animals across generations. **A** Schematic representation of the experimental setup. The *fzo-1* heterozygotes progeny of heteroplasmic hermaphrodites (*fzo-1(ht);+/\Delta*mtDNA) was identified and maintained using self-propagation and single worm genotyping to establish heteroplasmic lines carrying *fzo-1(ht);+/\Delta*mtDNA. Progeny animals (generation 1; G1) were isolated, allowed to lay eggs, and their genotypes were determined. Heteroplasmic mutant *fzo-1(mut);+/\Delta*mtDNA or wild type *fzo-1(wt);+/\Delta*mtDNA progeny were then monitored over several generations (G2m-G4m and G2wt-G4wt, respectively). **B** The percent of gravid adults of *fzo-1(mut);+/\Delta*mtDNA mutant progeny across generations (G1m-G4m) at the indicated times after egg laying (G1m $N = 3, n = 40$, G2m $N = 4, n = 152$, G3m $N = 3, n = 155$ and G4m $N = 3, n = 82$). Data were analyzed using Cox proportional-hazards regression (Additional file 1: Table S2). G2m and G3m were slower to reach adulthood than G1m ($P < 0.001$) but not G4m ($P = 0.750$). **C** The percent of hatched embryos of *fzo-1(mut);+/\Delta*mtDNA progeny across generations (G2m $N = 7, n = 236$, G3m $N = 6, n = 155$ and G4m $N = 4, n = 107$) and the stable line (> 20 generations) *fzo-1(mut);+/\Delta*mtDNA ($N = 4, n = 93$). Data are means ± 1 standard error of the mean (1SE). Data were analyzed using one-way ANOVA followed by a Tukey's post hoc test, (**) denotes $P < 0.002$ compared with G2m animals. **D, E** Box plot showing the percent of Δ mtDNA ($N > 3$ biological repeats) determined in individual animals (**D**) of the parental heteroplasmic strain *fzo-1(ht);+/\Delta*mtDNA ($n = 23$), the heteroplasmic *fzo-1(mut)* mutant cross-progeny strains (G1ht $n = 13$, G1m-G4m $n = 20, 31, 21$ and 21 , respectively) and the progeny of G4m animals crossed with *fzo-1(wt)*, (Gm \rightarrow Gwt $n = 21$); (**E**) of the heteroplasmic *fzo-1(wt)* cross progeny strains (G1wt-G4wt $n = 17, 20, 27$ and 21 , respectively). In the boxplot representation, center line, median; box limits, upper and lower quartiles; whiskers, minimum and maximum; points, data. Data were analyzed using Fractional regression (Additional file 1: Table S3). Δ mtDNA levels of G2m-G4m and Gm \rightarrow Gwt were significantly lower than those of the parental heteroplasmic strain *fzo-1(ht);+/\Delta*mtDNA, (**) denotes $P < 0.001$. **F** The percent of Δ mtDNA determined for a population of animals from the stable cross lines (> 20 generations), *fzo-1(wt);+/\Delta*mtDNA ($N = 7$), *fzo-1(mut);+/\Delta*mtDNA ($N = 3$) and *fzo-1(mut);+/\Delta*mtDNA; *fzo-1(Gm \rightarrow Gwt)* ($N = 4$). Data are means ± 1 standard error of the mean (1SE). Data were analyzed using one-way ANOVA followed by a Tukey's post hoc test, (**) denotes $P < 0.001$ compared with *fzo-1(wt);+/\Delta*mtDNA animals. Individual data values are presented in Additional file 2

Selection against heteroplasmic truncations depends on deletion size or mtDNA position

We next asked whether the deleterious interactions between *fzo-1(mut)* and Δ mtDNA depend on the size or genomic location of mtDNA deletions. To achieve this goal, we characterized two additional mtDNA deletions obtained from the Million Mutation Project strain collection [29]. Specifically, these deletions comprise two new stable heteroplasmic *C. elegans* strains: *bguDf1* (derived from strain VC40128), harboring a mixture of intact +mtDNA along with mtDNA molecules lacking ~1kb (1kb Δ mtDNA) encompassing two essential mtDNA genes (i.e., mt-ATP6 and mt-ND2) and three tRNAs (i.e., K, L, and S); the second strain, *bguDf2* (derived from VC20469), harbors in addition to the +mtDNA, a ~4.2kb mtDNA deletion (4kb Δ mtDNA) encompassing four different essential genes (i.e., mt-CO1, mt-CO2, mt-ND3, and mt-ND5) and five tRNAs (i.e., C, M, D, G, and H). Notably, the levels of the 1kb Δ mtDNA and 4kb Δ mtDNA were stable over >100 generations (80% and 55%, respectively) in the presence of functional (wild type) *fzo-1*. Reanalysis of whole-genome sequencing data for the two mutant strains identified +mtDNA and deletion sequences, as previously described [29, 30]. These analyses did not reveal any evidence for duplicated regions, confirming the mtDNA deletion heteroplasmy in these strains (Additional file 1: Fig. S3A-B). As previously observed for *uaDf5/+* [16], truncated mtDNA levels highly varied between animals, while intact +mtDNA levels were more constant (Additional file 1: Fig. S3C-D). The animals displayed neither embryonic nor developmental phenotypes, and no impact on mitochondria fusion was observed (Additional file 1: Fig. S3E-G and Table S2).

Heteroplasmic hermaphrodites of both strains were separately crossed with *fzo-1(mut)* heterozygote males, followed by self-cross of F1 progeny (cross as in Fig. 1A). Like the approach taken with the *uaDf5/+* strain, we examined the distribution of the genotypes in the F2 heteroplasmic progeny. We found that the genotypes distribution for the *fzo-1(mut);+/1kb Δ mtDNA* did not deviate from the expected Mendelian ratio (23.5% homozygous *fzo-1(mut)*, 43.2% *fzo-1(ht)* and 33.3% *fzo-1(wt)* ($P = 0.14$, chi-square test; Additional file 1: Table S1). In contrast, this ratio strongly deviated from the expected Mendelian ratio for *fzo-1(mut)* animals harboring +/4kb Δ mtDNA (6.4% homozygous *fzo-1(mut)*, 59.3% *fzo-1(ht)* and 34.3% *fzo-1(wt)* ($P < 0.001$, chi-square test; Additional file 1: Table S1). Hence, these results indicate that *fzo-1(mut)* differentially tolerates mtDNA deletions based on size and/or mtDNA position.

We next quantified the levels of Δ mtDNA in mutant versus wild type *fzo-1* progeny across four subsequent

generations (as in Fig. 2A; Fig. 3 and Additional file 1: Table S3). We found that both truncated mtDNA molecules were undetectable after four generations (Fig. 3A, B), yet the decline rates significantly diverged (Fig. 3C). Specifically, mean Δ mtDNA levels were significantly lower in *fzo-1(mut)* animals harboring the 4kb Δ mtDNA than in animals harboring either 1kb Δ mtDNA or 3kb Δ mtDNA in both G1m and G2m animals (fractional regression followed by within generation pairwise comparisons, $P < 0.001$; Fig. 3C and Additional file 1: Table S3). By the G3m generation, mean Δ mtDNA levels of 3kb Δ mtDNA were also significantly lower than those observed in animals harboring 1kb Δ mtDNA. Indeed, the 1kb Δ mtDNA was still detected in most of G3m animals ($N = 13/18$). It is worth noting that the levels of both types of Δ mtDNA did not significantly change across the G1wt-G4wt generations of the *fzo-1(wt);+/ Δ mtDNA* animals (fractional regression, $P > 0.118$ in both cases; Additional file 1: Fig. S3H-I and Table S3).

To assess whether the truncated mtDNAs were completely lost, we crossed G4m hermaphrodites with wild type males and isolated *fzo-1(wt)* progeny (Gm \rightarrow wt). qPCR analyses revealed no traces of the Δ mtDNA copies in subsequent generations (fractional regression, $P < 0.001$; Fig. 3A-B and Additional file 1: Table S3). Thus, disrupting *fzo-1* function resulted in a complete and specific loss of a variety of heteroplasmic Δ mtDNAs. We interpret these results to mean that *fzo-1* function is sensitive to either the size or location of deleterious mtDNA heteroplasmy.

Selection against Δ mtDNA molecules occurs during *C. elegans* development

In *C. elegans*, mtDNA copy numbers increase significantly during the fourth larval stage (L4) in association with oocyte production [27, 31]. We, therefore, asked at which point during the *C. elegans* life cycle selection against Δ mtDNA occurred. Given that the relative levels of Δ mtDNA are maintained during normal development [27], we compared Δ mtDNA levels between embryos and adults in G2m animals. Our results indicate that Δ mtDNA levels were dramatically reduced (~5-fold) during the development of G2m animals (ANOVA followed by a Tukey's post hoc test, $P < 0.001$; Fig. 4A) but not in G2wt animals (Fig. 4B). This observation suggests that Δ mtDNA is most likely selected against during the *fzo-1(mut)* worm development, in agreement with the observed adverse effect of heteroplasmy on the hatching and development of G2m animals.

To examine the possible association of Δ mtDNA levels with embryo lethality, we compared Δ mtDNA levels of unhatched embryos (unhatched >48 h after being laid) to newly hatched larvae (L1). As expected, given

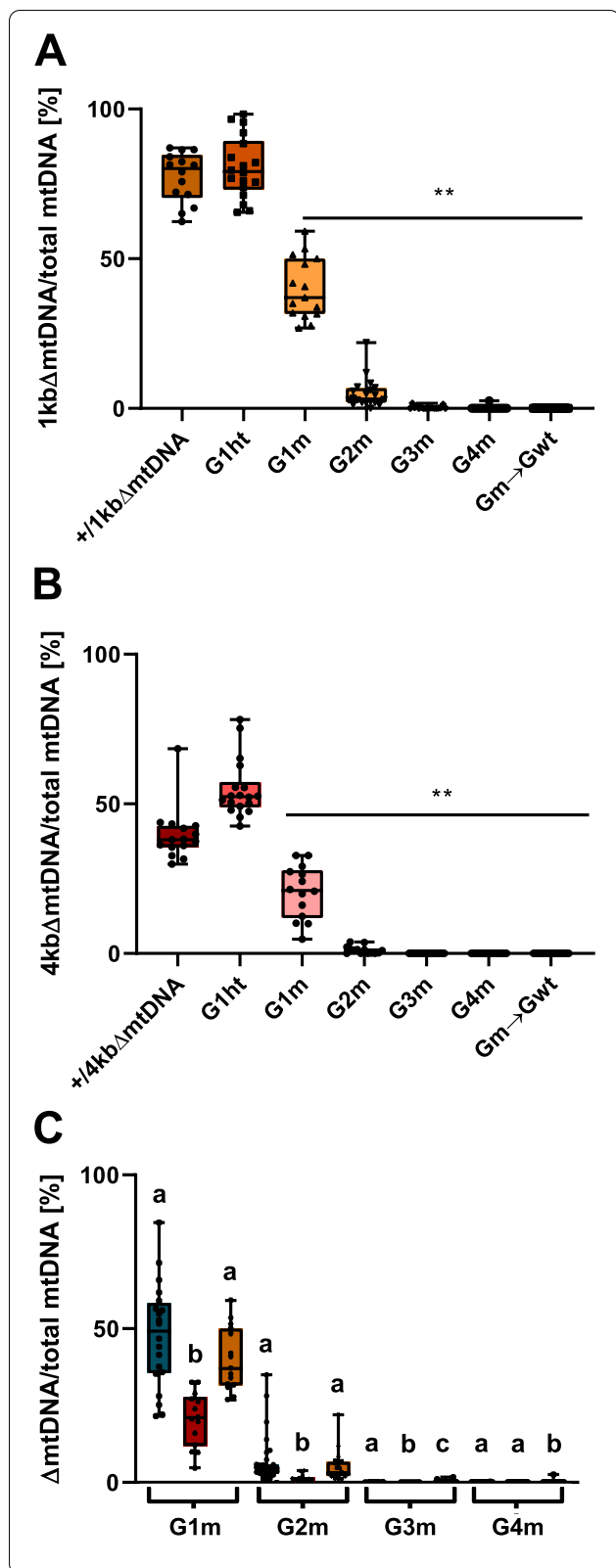
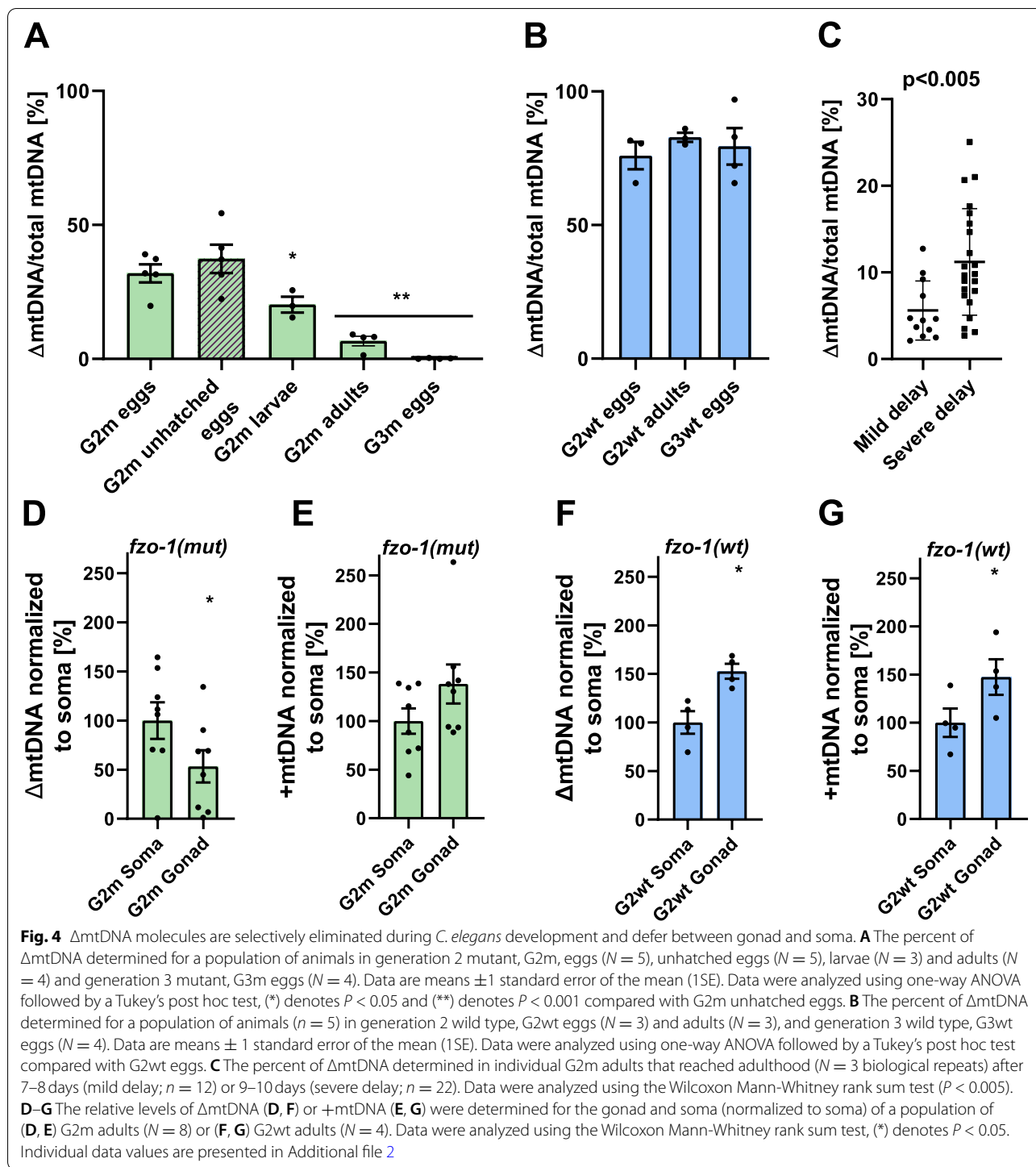


Fig. 3 ΔmtDNA levels are differentially eliminated in *fzo-1(mut);ΔmtDNA* animals based on size or mtDNA position. **A, B** Box plot showing the percentage of 1kbΔmtDNA (**A**) or 4kbΔmtDNA (**B**) ΔmtDNA ($N > 3$ biological repeats), determined in individual animals of the parental heteroplasmic strain +/1kbΔmtDNA ($n = 14$) and +/4kbΔmtDNA ($n = 15$), the *fzo-1(mut)* mutant cross-progeny strains (1kbΔmtDNA F1(ht) $n = 18$, G1m-G4m $n = 15, 20, 17$ and 19 and 4kbΔmtDNA F1(ht) $n = 18$, G1m-G4m $n = 14, 14, 21$ and 20) and the progeny of G4m animals crossed with *fzo-1(wt)*, (Gm → Gwt $n = 15$ and $n = 20$ respectively). In the boxplot representation, center line, median; box limits, upper and lower quartiles; whiskers, minimum and maximum; points, data. Data were analyzed using fractional regression (Additional file 1: Table S3). ΔmtDNA levels of G1m-G4m and Gm→Gwt were significantly lower than those of the parental strains in both +/1kbΔmtDNA and +/4kbΔmtDNA, (**) denotes $P < 0.001$. **C** Box plot comparing the percentage of ΔmtDNA in animals carrying +/3kbΔmtDNA (blue), +/1kbΔmtDNA (yellow) or +/4kbΔmtDNA (red) in each generation (G1m-G4m; data from Fig. 2C, Fig. 3A, and Fig. 3B, respectively). In the boxplot representation, center line, median; box limits, upper and lower quartiles; whiskers, minimum and maximum; points, data. Data were analyzed using fractional regression followed by within generation pairwise comparisons (Additional file 1: Table S3), different letters indicate a significant difference in mean levels of ΔmtDNA levels: G1-G2, 4 kb levels (a) lower than 3 kb and 1 kb (b, $P < 0.001$); G3, 4 kb levels (a) lower than 3 kb (b, $P < 0.01$) and 4 kb (a) and 3 kb (b) levels lower than 1 kb (c, $P < 0.001$); G4, 4 kb and 3 kb levels (a) lower than 1 kb (b, $P < 0.001$). Individual data values are presented in Additional file 2

that ~85% of G2 embryos did not hatch, ΔmtDNA levels of unhatched embryos were similar to the relative ΔmtDNA levels of newly laid embryos. In contrast, ΔmtDNA levels in L1 animals were reduced by 2-fold (ANOVA followed by a Tukey’s post hoc test, $P < 0.05$; Fig. 4A). This suggests that hatching is enabled only in embryos with reduced ΔmtDNA levels.

We next examined whether ΔmtDNA levels associate with developmental delay. To this end, we compared the levels of ΔmtDNA in mildly delayed G2 animals that reached adulthood on days 7–8 to severely delayed animals that reached adulthood on days 9–10. Our results show that ΔmtDNA levels were 2-fold higher in the severely delayed group (Wilcoxon Mann-Whitney rank sum test, $P < 0.005$ test; Fig. 4C). These data demonstrate increased embryo lethality and aggravation in developmental delay in animals harboring high levels of ΔmtDNA. This supports our interpretation that disruption of mitochondrial fusion in animals carrying ΔmtDNA molecules leads to reduced fitness and suggests that there is selection against such molecules at the level of the organism.



Selection against Δ mtDNA molecules defers between gonad and soma

Previously Lieber et al. demonstrated germline selection acting against high levels of mutant mtDNA in *Drosophila* oogenesis [22]. In *C. elegans*, the germline tends to accumulate higher levels of deleterious mitochondrial

molecules than somatic tissues, although unfertilized oocytes contain lower levels of Δ mtDNA compared to that of germline tissue [32]. Consistently, we found that Δ mtDNA molecules became undetectable in the resultant embryos of G2m animals (i.e., in G3m animals; Fig. 4A). Hence, it is possible that selection against

Δ mtDNA molecules occurred during *C. elegans* gametogenesis. In support of this claim, a comparison of Δ mtDNA levels between gonads and somatic tissues in G2m animals revealed a two-fold decrease of Δ mtDNA levels in the gonads (Wilcoxon Mann-Whitney rank sum test, $P < 0.05$; Fig. 4D), whereas the levels of +mtDNA intact molecules were ~ 1.4 -fold higher in the gonad (Fig. 4E). In contrast, both Δ mtDNA and +mtDNA molecules were ~ 1.5 -fold higher in the gonad when comparing gonads and somatic tissues of *fzo-1(wt);+/ Δ mtDNA* animals ($P < 0.05$ Wilcoxon Mann-Whitney rank sum test; Fig. 4F, G) [32]. Since both the *Drosophila* experiments [12, 21, 22] and our observations are consistent, we argue that selection against Δ mtDNA molecules during gametogenesis is evolutionarily conserved [12].

PARKIN mutant aggravates the adverse effects of the Δ mtDNA-*fzo-1* interactions

Since Parkin mediates the turnover of mitofusins and hence impacts their activity [33, 34], we asked what would be the impact of the *pdr-1*;*fzo-1* double mutant on the inheritance of the Δ mtDNA. To address this question, we first crossed +/ Δ mtDNA heteroplasmic hermaphrodites with *pdr-1(gk448)* (here named *pdr-1(mut)*) males and established a stable *pdr-1(mut);+/ Δ mtDNA* strain. Consistent with previous findings, the Δ mtDNA levels were elevated in this strain (75%) [14–17]. To establish a strain which is mutant in *pdr-1* and *fzo-1* in the context of +/ Δ mtDNA heteroplasmy, we then crossed *pdr-1(mut);+/ Δ mtDNA* heteroplasmic hermaphrodites with *pdr-1*;*fzo-1* heterozygous males, let the F1 progeny self-cross, and isolated *fzo-1(ht);pdr-1(mut)* hermaphrodites that are harboring +/ Δ mtDNA (Fig. 5A). This strain was allowed to propagate, and the genotypic distribution of the heteroplasmic progeny was assessed. While the genotype distribution of *fzo-1(mut);+/ Δ mtDNA* did not deviate from the expected Mendelian ratio, the genotype distribution of *fzo-1(ht);pdr-1(mut);+/ Δ mtDNA* was strongly affected, as follows: 9% homozygous *fzo-1(mut);pdr-1(mut)*, 55.8% *fzo-1(ht);pdr-1(mut)*, and 35.2% *fzo-1(wt);pdr-1(mut)* ($P < 0.001$, chi-square test; Additional file 1: Table S1). This suggests that the heteroplasmic Δ mtDNA cannot be tolerated in the background of *fzo-1(mut);pdr-1(mut)* double mutant, as reflected in further reduction in fitness.

We next monitored the development and fecundity of these animals. Phenotypic characterization revealed a developmental delay in the *fzo-1(mut);pdr-1(mut);+/ Δ mtDNA* G1m, similar to the parental strain (11/11 were adults by day 7); and most of the G1m progeny (G2m eggs) hatched ($85 \pm 8\%$; Additional file 1: Fig. S4A). However, $66 \pm 1\%$ of the G2m were developmentally arrested (Additional file 1: Fig. S4B). Only $33 \pm 12\%$

of the remaining animals reached adulthood by day 7 (Cox proportional-hazards regression, $P < 0.001$; Fig. 5B and Additional file 1: Fig. S4C and Table S2), and their progeny production was severely reduced (laying seven eggs or less over 20h). Moreover, $22 \pm 7.5\%$ of the G3m animals were still developmentally arrested (Additional file 1: Fig. S4B), and G3m development was similarly delayed (Cox proportional-hazards regression, $P < 0.001$; Fig. 5B and Additional file 1: Fig. S4C and Table S2). However, we noticed a significant recovery of animals' development during subsequent generations (Fig. 5B and S4C). In contrast, heteroplasmic *fzo-1(wt);pdr-1(mut);+/ Δ mtDNA* hatching and development was unaffected ($\sim 98\%$ hatched and 100% were adults by day 7; Additional file 1: Fig. S4A and S4C). Thus, the adverse effects of the interaction between *fzo-1(mut)* and Δ mtDNA on fecundity and developmental timing were aggravated by *pdr-1(mut)*, supporting *fzo-1-pdr-1* epistasis.

We next asked whether the selection against Δ mtDNA would strengthen in the background of *fzo-1(mut);pdr-1(mut);+/ Δ mtDNA*. To directly examine this, we compared the levels of Δ mtDNA molecules in *fzo-1(mut);pdr-1(mut);+/ Δ mtDNA* animals (Fig. 5C) to *fzo-1(mut);+/ Δ mtDNA* (Fig. 2D) across G1m–G4m generations. We found that Δ mtDNA levels declined more sharply in *fzo-1(mut);pdr-1(mut);+/ Δ mtDNA* as compared to the single mutant strain *fzo-1(mut);+/ Δ mtDNA*. Specifically, we found lower Δ mtDNA levels in G1m and G2m *fzo-1(mut);pdr-1(mut);+/ Δ mtDNA* animals (fractional regression followed by within generation pairwise comparisons, $P < 0.001$; Additional file 1: Table S3). In contrast, Δ mtDNA levels did not significantly change across generations of *fzo-1(wt);pdr-1(mut);+/ Δ mtDNA* animals (fractional regression, $P > 0.167$ in all cases; Additional file 1: Fig. S4D and Table S3). Taken together, the concomitant disruption of fusion and mitophagy strongly selected against Δ mtDNA molecules. In support of this interpretation, we noticed that even in the *fzo-1(ht);pdr-1(mut);+/ Δ mtDNA* animals, where only one genomic copy of *fzo-1* remained functional, Δ mtDNA levels declined and in some individuals were lost across ~ 25 generations (Wilcoxon Mann-Whitney rank sum test, $P < 0.001$; Fig. 5D).

Finally, we asked whether impaired mitophagy affects selection against Δ mtDNA in the worm germline. To this end, we examined the ratio of Δ mtDNA and +mtDNA between the gonad and soma in double mutant *fzo-1(mut);pdr-1(mut);+/ Δ mtDNA* animals (Fig. 5E, F) and *pdr-1(mut);+/ Δ mtDNA* (Fig. 5G, H). While mtDNA levels, including both Δ mtDNA and +mtDNA, were ~ 1.5 -fold higher in the gonad vs. the soma of *pdr-1(mut)* animals (Wilcoxon Mann-Whitney rank sum test, $P < 0.05$; Fig. 5G, H), similar to wild type animals

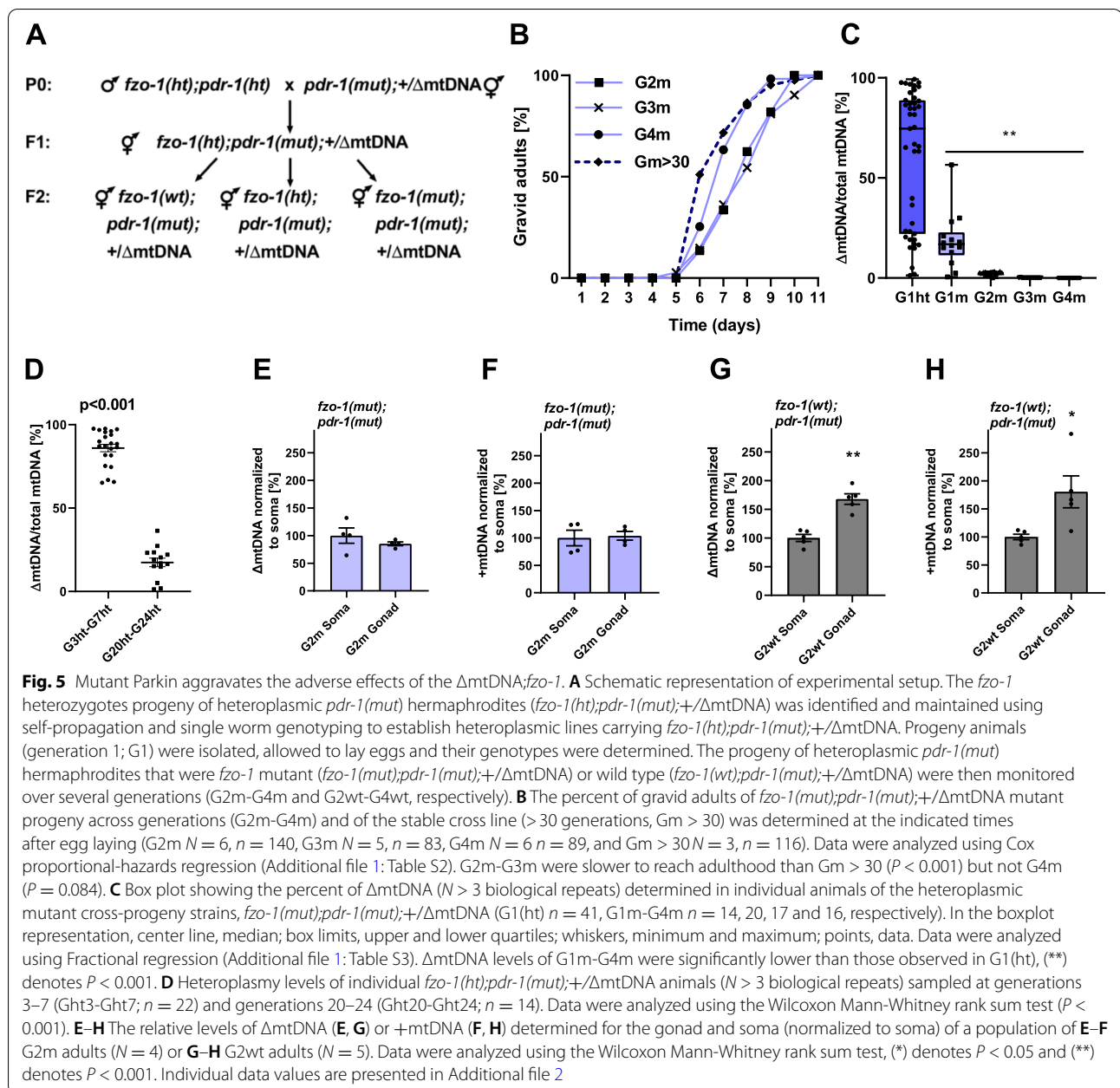


(Fig. 4F, G). We observed that *fzo-1(mut);pdr-1(mut);+ΔmtDNA* animals displayed similar mtDNA levels in the gonad compared to soma, for both truncated and intact mtDNA molecules (Fig. 5E, F). On top of the selection against Δ mtDNA, *fzo-1(mut);pdr-1(mut);+ΔmtDNA* double mutant displayed a reduction in total mtDNA levels, again supporting epistasis. Taken together, these data suggest that disrupting parkin-mediated mitophagy increased the organismal selection in *fzo-1(mut);pdr-1(mut);+ΔmtDNA* individuals, which is associated with reduced fitness.

Discussion

Our cross-generational analyses revealed complete loss of heteroplasmic deleterious mtDNA deletions when mitochondrial fusion is compromised. This demonstrated that heteroplasmy of deleterious mtDNA molecules could not be tolerated unless in the presence of a functional compensatory mechanism inherent to the mitochondrial network and the mitochondrial quality control machinery [14–16, 22, 23]. What drives this selection? It was previously found that *fzo-1* mutation impacted the developmental pace of the worms [35–37]. Nevertheless, we

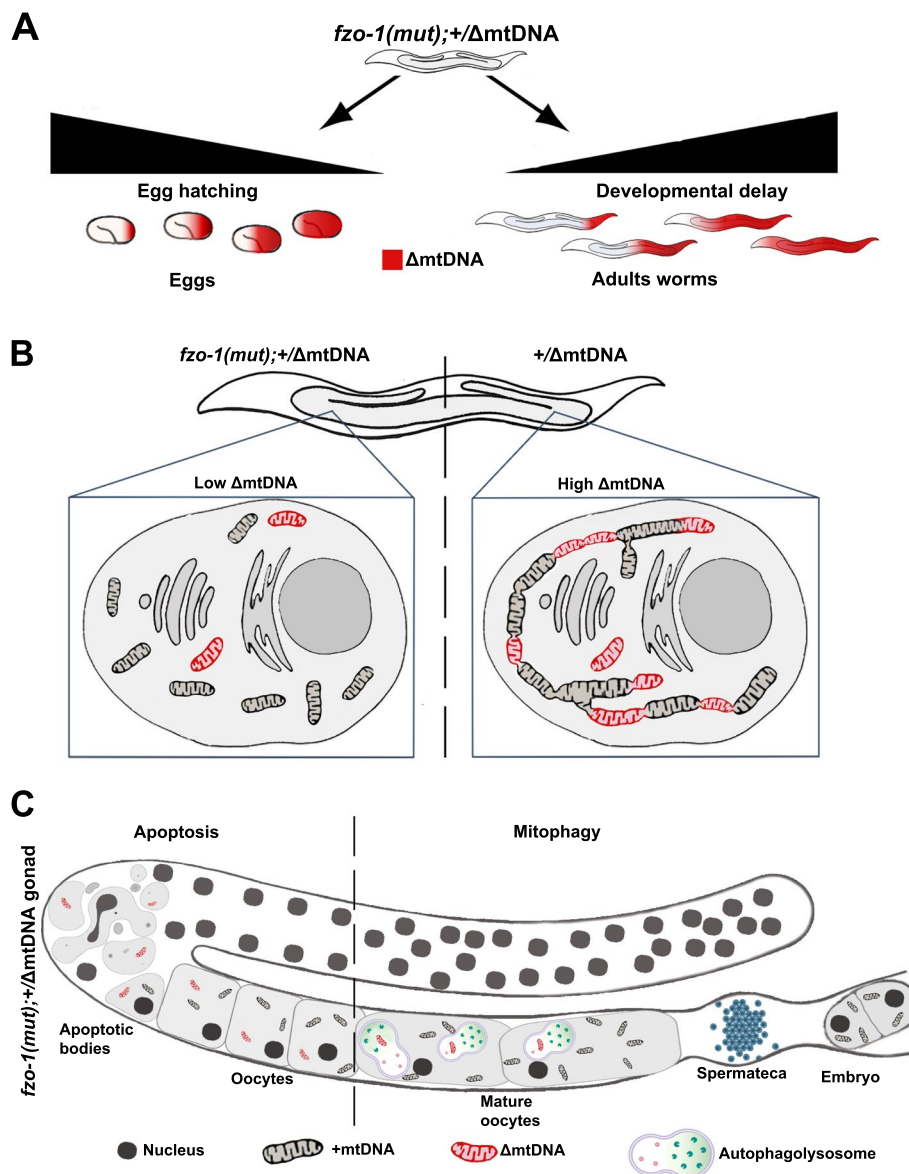


Fig. 6 A model depicting selective removal of Δ mtDNA during development and gametogenesis of *C. elegans*. **A** Schematic representation—high Δ mtDNA levels (red) associate with reduced egg hatching and delayed development. **B** Schematic representation of mitochondria in the gonad, carrying intact $+$ mtDNA (black) and Δ mtDNA (red). Mitochondria in *fzo-1(wt)* oocytes form an intracellular mitochondrial network suggested to enable mitochondrial functional complementation, hence allowing Δ mtDNA inheritance. In contrast, in *fzo-1(mut)* animals, the fusion machinery is compromised, mitochondria are fragmented, suggesting that Δ mtDNA molecules are ‘exposed’ and hence selectively eliminated in the gonad of *fzo-1(mut);+ΔmtDNA*. **C** Two possible non-mutually exclusive mechanisms can explain the selective removal of Δ mtDNA molecules in the gonad of *fzo-1(mut);+ΔmtDNA*. Signals from mitochondria are suggested to trigger programmed cell death of germ cells when the transition from a globular to a tubular organization is disrupted, as in *fzo-1(mut)* (left). Sperm-derived signals are suggested to trigger lysosome acidification in mature oocytes, which can activate mitophagy (right). These processes can selectively impact the removal of mitochondria with high levels of Δ mtDNA, respectively, in *fzo-1(mut)* animals. The figure was created in part using BioRender.com

show that introducing heteroplasmic mtDNA deletions strongly aggravated these phenotypes, leading to a sharp decline in survival and fecundity. This was manifested by increased embryonic lethality and delayed or even arrested larval development of worms with high levels of

deleterious heteroplasmic mtDNAs (Fig. 6A). This strong selective pressure also positively correlated with the decline in heteroplasmic deletion levels across generations. Since the loss of Δ mtDNA molecules is associated with the improved health condition of the worms within

3–4 generations, mitochondrial fusion is likely critical for tolerating Δ mtDNA molecules to maintain fitness.

In parallel, our discovery that the levels of heteroplasmic deletions are specifically reduced in the gonad when the fusion machinery is impaired (Fig. 6B) is consistent with previous findings of selective forces in the human germline [4, 5, 12]. Moreover, in *Drosophila*, germline selection of heteroplasmic mutations was directly observed in response to compromised fusion and quality control machinery [12, 21, 22]. We found that disrupting mitophagy in addition to mitochondrial fusion (*fzo-1(mut);pdr-1(mut)*) in the presence of Δ mtDNA sharply increased lethality already in G1 animals (reflected by the deviation from Mendelian ratios). Likewise, we found that disrupting Parkin-mediated mitophagy did not block germline selection, affecting the specific removal of mtDNA. These findings agree with germline selection in *Drosophila*, where downregulation of mitophagy factors, BNIP3 and Atg1, significantly blocked selection against fragmented mitochondria in germline cysts [22]. We, therefore, propose that selection against deleterious mtDNA molecules across generations affects the fitness of the organism, at two levels, namely during embryogenesis and larvae development as well as during oogenesis (Fig. 6A, B).

Two quality control processes were previously suggested to impact germline health and may contribute to selection against mutated mtDNA in *fzo-1(mut)* animals. Firstly, increased apoptosis was observed upon disruption of mitochondrial transition from a globular to a tubular organization in *C. elegans* oogenesis [38]. This may contribute to selective mitochondrial removal since selective export of mitochondria from germ cells undergoing apoptosis was observed [39]. Secondly, sperm-derived signals were found to induce lysosome acidification in mature oocytes prior to fertilization [40] and could promote mitophagy activation of fragmented mitochondria in *fzo-1(mut)* animals (Fig. 6C). Compromising either of these two processes led to reduced brood size. Therefore, we argue that the interaction between mitochondrial fusion and quality control machinery is not only critical to cope with Δ mtDNA within the cell but is essential for the organism's fecundity, development, and survival across generations. Other selection mechanisms, such as selective replication, observed in *Drosophila* [12], or homologous recombination of a deletion and a corresponding duplication (in case of "triploidy") [41] could also contribute to selection against mutated mtDNA in *C. elegans*. Our results suggest that the latter explanations are less likely for the heteroplasmic strains described in this study.

Our analysis of three different mtDNA deletions in *C. elegans* revealed significant differences in the pace of

their loss and levels of phenotypic severity when grown in the presence of a *fzo-1* mutant. Indeed, these three deletions differ in size and encompass different sets of mtDNA genes and tRNAs, suggesting that the fusion machinery is sensitive to differential severity of the phenotypic impact of heteroplasmic mutations. This finding is in line with differences in the penetrance of disease-causing mutations, which range between 60 and 80%, depending on the symptoms [9]. Nevertheless, the question about the functional importance of certain mtDNA regions versus others remains open. This calls for a screen of mtDNA mutants that will systematically enable assessing the sensitivity of the mitochondrial quality control and fusion machinery in differentiating the phenotypic impact of a variety of mutations, locations, and sizes.

If mitochondrial fusion is indeed important for modulating the inheritance of mtDNA heteroplasmy, one could anticipate that dysfunctional mitochondrial fusion, such as in the case of Charcot Marie Tooth type 2A (CMT2A) patients, will affect patterns of heteroplasmy. Our deep mtDNA sequencing analysis of three CMT2A pedigrees lends first clues that this might be the case [42]. Whereas two of the pedigrees did not reveal any potentially functional mtDNA mutations or deletions, we found that the levels of a potentially functional mtDNA mutation in a patient were notably lower than her healthy maternal relatives. We note that these results are in line with the observations in worms, supporting our working hypothesis that the fusion machinery modulates the levels of deleterious mtDNA heteroplasmy across generations to allow tolerance and survival. However, there are two mitofusin genes (MFN1 and MFN2) in humans, and MFN2 as well as DRP1 (inner membrane fusion) also function as tethers at mitochondria-associated ER membranes [43, 44] and could impact Parkin-mediated mitochondrial quality control [34, 45, 46]. Future collection of a larger number of CMT2A pedigrees is required to draw clearer conclusions.

The complete loss of Δ mtDNA across *C. elegans* generations underlines the fusion machinery as an attractive candidate target for future treatment of mitochondrial disorders. For example, the activity of protein quality control systems, including this machinery, declines during the aging of the individual [47, 48], and the levels/repertoire of mtDNA heteroplasmic deletions increase in tissues from aged individuals [49]. It would, therefore, be of great interest to assess the importance of such three-way interaction (i.e., mitochondrial fusion-mitochondrial quality control and patterns of heteroplasmy) to the tendency to develop age-associated diseases.

Conclusions

Here, by manipulating the fusion machinery in *C. elegans*, we demonstrated that *fzo-1* (mitofusin) is a key modulator of mtDNA heteroplasmy while showing its impact on the transmission of heteroplasmic deletions across generations in living animals. Firstly, we discovered that a *fzo-1(mut)* led to the complete loss of three different mtDNA deletions, separately. These findings provide experimental support for the hypothesis that functional complementation among mitochondria in the intracellular network likely enables the survival and prevalence of deleterious heteroplasmic mtDNA mutations in the population [25, 26]. Secondly, we found that the *fzo-1(mut)* was differentially sensitive to the size/nucleotide positions of the different mtDNA deletions. Third, *fzo-1(mut);pdr-1(mut)* double mutants selected against the survival of animals with heteroplasmic Δ mtDNA deletion and accelerated the loss of Δ mtDNA molecules across generations. Taken together, our results demonstrate the importance of cross-talk between mitochondrial fusion and the mitochondrial quality control machinery in protecting living animals from the adverse impact of inheriting deleterious mtDNA molecules.

Methods

Nematodes and growth conditions

A list of strains used in this work and name abbreviations are found in Additional file 1: Table S4. All strains were outcrosses to our N2 stock at least four times. Nematodes were grown on Nematode Growth Medium (NGM) plates seeded with the *Escherichia coli* OP50-1 strain at 15 °C.

Statistical analyses

To test the null hypothesis that the heteroplasmic deletions reduce the fitness of WT (Additional file 1: Figs. S2B and S3E), *fzo-1(mut)* (Fig. 1B, C and Fig. 2C) or *fzo-1(mut);pdr-1(mut)*; (Additional file 1: Fig. S4A-C) as compared to wild type or *fzo-1(mut)* animals, we used one-way analysis of variance (ANOVA) followed by a Tukey's post hoc test. We used the same test to compare the levels of Δ mtDNA, +mtDNA, and TMRE staining in *fzo-1(mut)* and *fzo-1(wt)* strains (Fig. 2F, Fig. 4A, B, and Additional file 1: S1B). Data are presented as bar graphs showing means \pm 1 standard error of the mean (1SE). To compare the mtDNA (Δ mtDNA and/or +mtDNA) levels between two conditions and assess statistical significance (Fig. 4C–G, Fig. 5D–H, and Additional file 1: S3C–D), we used the Wilcoxon Mann-Whitney rank sum test. Data are presented as scatter dot plots showing points for data or bar graphs showing means \pm 1SE. To test whether heteroplasmic progeny deviated from

the expected Mendelian ratio, we used χ^2 goodness of fit test, data are presented in Additional file 1: Table S1. To examine differences in developmental rate across generations of *fzo-1* mutant (Figs. 2B and 5B) or wild type animals (Additional file 1: Figs. S2A and S3F), we used Cox proportional-hazards regressions (Additional file 1: Table S2). To control for the dependency of individuals within biological repeats, a robust jackknife variance estimator grouped by observations per experimental plate was used. Data points showing the percent of total animals that reached adulthood within the experimental time (11 days) are presented as line graphs. To test for changes in heteroplasmic deletions (Fig. 2D, E, Fig. 3A, B, Fig. 5C, and Additional file 1: S3H–I, S4D) or +mtDNA (Additional file 1: Fig. S2C–D) levels across generations of *fzo-1* mutant (Fig. 2D, Fig. 3A, B, Fig. 5C, and Additional file 1: S2C) or wild type animals (Fig. 2E and Additional file 1: S2D, S3H–I, and S4D), we used fractional regressions with logit link function (Additional file 1: Table S3). To compare the change in heteroplasmic deletion levels across generations in the different genetic backgrounds (Fig. 3C), we used a fractional regression with logit link function followed by within generation pairwise comparisons (Additional file 1: Table S3). To control for the dependency of individuals within biological repeats, a robust variance estimator grouped by observations per experimental plate was used. Odds ratios were calculated to determine the likelihood of heteroplasmy in a given generation. Data are presented in box plot representation: center line, median; box limits, upper and lower quartiles; whiskers, minimum and maximum; points, data. The numbers of biological repeats (N) and individuals (n) in each condition tested are noted in the figure legends (Figs. 1, 2, 3, and 5 and Additional file 1: S1–S4).

Single worm genotyping

Animal genotype was determined using a single worm PCR Phire Animal Tissue Direct PCR Kit (Thermo Scientific) with primers to detect *fzo-1* or *pdr-1* deletions. The list of PCR primers is found in Additional file 1: Table S5. The resultant amplification products were visualized by gel electrophoresis to determine the genotype.

Establishing and maintaining *fzo-1* heterozygotes heteroplasmic lines

Mutant *fzo-1(tm1133)* animals (strain CU5991) are very poor in mating and, therefore, were first crossed with males expressing a yellow fluorescent protein marker (*unc-54p::YFP*). Heteroplasmic hermaphrodites (*uaDf5/+*, *bguDf1/+* or *bguDf2/+*) were then crossed with *fzo-1(tm1133);unc-54p::YFP* heterozygote males to ensure maternal inheritance of mtDNA deletions (Fig. 1A). Heteroplasmic (*uaDf5/+*, *bguDf1/+*

or *bguDf2/+*) animals that were heterozygotes for *fzo-1(tm1133)*, *fzo-1(ht)*, were identified and maintained using single worm genotyping, establishing independent heteroplasmic lines carrying *fzo-1(ht)*.

Mutant *pdr-1(gk448)* animals (strain VC1024) were first crossed with heteroplasmic hermaphrodites (*uaDf5/+*) and with *fzo-1(tm1133)* to establish double mutant strains. *fzo-1(tm1133);pdr-1(gk448)* double mutants were crossed with *unc-54p::YFP* (marker); then, the F1 heterozygote males, *fzo-1(tm1133);pdr-1(gk448);unc-54p::YFP*, were crossed with heteroplasmic hermaphrodites, Δ mtDNA;*pdr-1(gk448)* to ensure maternal inheritance of *uaDf5* (Fig. 5A). Heteroplasmic (*uaDf5/+*) animals that were homozygous to *pdr-1(gk448)*, *pdr-1(mut)*, and heterozygotes for *fzo-1(tm1133)*, were identified using PCR genotyping. *fzo-1(ht)* were then maintained using single worm genotyping to establish a heteroplasmic line carrying *fzo-1(ht);pdr-1(mut)*.

Monitoring animals across generations

Single animals from the heterozygotes heteroplasmic lines (*uaDf5/+*, *bguDf1/+*, or *bguDf2/+*) were isolated, allowed to lay eggs, and genotyped using a single worm PCR for *fzo-1*. The progeny of *fzo-1(ht)* was again isolated, allowed to lay eggs, and screened to identify mutant or wild type *fzo-1* animals (G1m and G1wt, respectively). Heterozygous progeny was maintained to generate G1. The progeny of mutant or wild type animals (G2m and G2wt, respectively) was then monitored and/or isolated and allowed to lay eggs. This was repeated over several generations (G2m-G4m and G2wt-G4wt, respectively; Fig. 2A).

To test for residual Δ mtDNA (*uaDf5*, *bguDf1*, or *bguDf2*), G4m hermaphrodites were crossed with wild type males; the progeny was allowed to self-propagate, isolated, allowed to lay eggs, and genotyped. Heteroplasmy levels in *fzo-1(wt)* animals (Gm→Gwt) were then examined.

Embryo hatching

Gravid animals were moved to a fresh plate for 2–12 h and then removed from the plates. Hatching was examined after 48 h. The numbers of biological repeats (*N*) and individuals examined (*n*) in each condition tested are noted in the figure legends (Fig. 1B, Fig. 2C and Additional file 1: S2B, S3E and S4A). Individual data values are included in Additional file 2.

Developmental timing

Single embryos were placed on fresh plates and allowed to grow at 15 °C. The animals' developmental stage was examined every day, and the number of animals reaching reproductive adulthood on each day was recorded.

Developmentally arrested animals that did not reach adulthood in over 11 days were excluded. The numbers of biological repeats (*N*) and individuals examined (*n*) in each condition tested are noted in the Figure legends (Fig. 1C, Fig. 2B, Fig. 5B and Additional file 1: S2A, S3F and S4B–C). Individual data values are included in Additional file 2.

Mitochondria staining and membrane potential assay

Age-synchronized adults were placed on NGM plates seeded with the *E. coli* OP50-1 and containing 100 μ M MitoTracker Deep Red FM (ThermoFisher) or 100 μ M TMRE (tetramethylrhodamine, ethyl ester) (Biotum). The animals were kept on the plates for 24 h in the dark and then recovered on regular plates for 2 h. Animals were then fixed with 4% paraformaldehyde and imaged using a LEICA DM5500 B epifluorescence microscope. MitoTracker was imaged using a $\times 40$ or a $\times 60$ numerical aperture objective with a 633-nm line for excitation. TMRE was imaged using a $\times 10$ numerical aperture objective with a 549-nm line for excitation. TMRE staining was quantified using CellProfiler cell image analysis software. The numbers of individuals examined (*n*) in each condition tested are noted in the figure legend of Additional file 1: S1B. Individual data values are included in Additional file 2.

DNA purification and extraction

Total DNA was extracted using a QuickExtract kit (Lucigen). Unless otherwise indicated, DNA was extracted from a single worm. When populations were examined, ~5 animals were collected. For embryos, DNA was extracted from 15 to 30 embryos. For gonad-soma analysis, gonads were dissected from 5 to 10 animals per biological repeat. DNA was extracted separately from the gonads and soma.

Quantification of mtDNA copy numbers

mtDNA levels were measured by qPCR performed on a C1000 Thermal Cycler (Bio-Rad) with KAPA SYBR-FAST qPCR Master Mix (KAPA Biosystems). Analysis of the results was performed using CFX Manager software (Bio-Rad). To quantify the different mtDNA molecules, three sets of primers were used for truncated (Δ mtDNA), intact (+mtDNA), and total mtDNA molecules for each of the three deletions examined (Additional file 1: Table S5). Δ mtDNA levels were determined using primers located in the boundaries of the deletions and thus amplified only from the truncated copies. +mtDNA levels were determined using one primer located within the deletion and a second primer located outside of the deletion and thus amplified only from the intact copies. Total mtDNA levels were determined

using primers located outside of the deletion area. For each sample, the average C_T (threshold cycle) of triplicate values obtained for these mtDNA molecules was normalized to a nuclear DNA marker using the $2^{-\Delta\Delta C_T}$ method [50]. Truncated/total or intact/total ratio was defined as the ratio of the normalized C_T values of truncated to total mtDNA for a given animal or strain. The numbers of biological repeats (N) and individuals examined (n) in each condition tested are noted in the figure legends (Figs. 2D–F, 3A, B, 4A–G and 5C–H and Additional file 1: S2C–D, S3C–D, S3H–I and S4D). Individual data values are included in Additional file 2.

Reanalysis of whole-genome sequencing

The occurrence of deletions and duplications in the mtDNA was assessed by analyzing whole-genome sequencing reads from the NCBI's Sequence Read Archive (SRA) database, corresponding to two of the strains used in this study: SRR801606 - SRR801609 for strain VC40128, and SRR793379 - SRR793382 for strain VC20469 [30]. Reads were downloaded, trimmed according to quality scores (default parameters), and filtered for excluding read-through adapters sequences. The processed reads were mapped against the entire genome of the N2 wild type strain to exclude contamination of nuclear mitochondrial DNA (NUMTs) in our results. N2 genome information was downloaded from NCBI's RefSeq database (accession numbers: Chr_1 - NC_003279.8, Chr_2 - NC_003280.10, Chr_3 - NC_003281.10, Chr_4 - NC_003282.8, Chr_5 - NC_003283.11, Chr_X - NC_003284.9, and Chr_M - NC_001328.1). We used a genome browser to visualize reads coverage and detect the previously reported deletions in the examined strains [29]. Deletions and duplications were determined by two parameters; a relative change in sequencing coverage and the mapping of broken read pairs at the edges of the deletions (i.e., new sites formed by the deletion or duplication). The algorithm would identify pairs as broken if the observed distance post mapping between the pairs was significantly larger than the expected distance, according to the size selection procedure during library preparation. Analyses described above were performed using CLC Genomics workbench 20, QIAGEN.

Gonad dissection

G2 wild type or mutant animals were placed in a drop of ultra-pure water on a coverslip slide, and a 25-gauge needle was used to remove the gonads from the body of the

animals. Gonads or the remaining carcasses were then transferred to a DNA extraction buffer.

Supplementary Information

The online version contains supplementary material available at <https://doi.org/10.1186/s12915-022-01241-2>.

Additional file 1: Table S1. Genotypes distribution of F2 progeny in different heteroplasmic strains. **Table S2.** Cox proportional-hazards regression analyses. **Table S3.** Fractional regression analyses. **Table S4.** A list of *C. elegans* strains used in this study. **Table S5.** A list of primers used in this study. **Figure S1.** Characterization of $\pm\Delta$ mtDNA animals. **Figure S2.** Characterization of *fzo-1(wt);+\Delta*mtDNA animals. **Figure S3.** Characterization of the 1kb Δ mtDNA and 4kb Δ mtDNA animals. **Figure S4.** Characterization of *fzo-1(wt);pdr-1(mut);+\Delta*mtDNA animals.

Additional file 2. Individual data values. Spreadsheets of numerical data for Figures 1, 2, 3, 4 and 5 and Supplementary Figures S1–S4.

Acknowledgements

Strains, CU5991, VC1024, and LB138 (after outcrossing ABZ271, ABZ283, and ABZ270, respectively), were provided by the *Caenorhabditis* Genetics Center, which is funded by the NIH National Center for Research Resources (NCRR). Strains, VC40128 and VC20469 (after outcrossing ABZ275 and ABZ279, respectively), were provided by the *C. elegans* Reverse Genetics Core Facility at the University of British Columbia, which is part of the international *C. elegans* Gene Knockout Consortium.

Authors' contributions

Conceptualization, A.B. and D.M.; experimental design, A.B. L.M., and I.V.; data acquisition, L.M., D.K., T.N., M.K., and S.D.; data analysis, L.M., D. B. T. C., C.J.K., J.M.V., Y.N., S. Z, and O.O.; writing and revising the text, A.B. and D.M. All authors read and approved the final manuscript.

Funding

This study was funded by the Israel Science Foundation (ISF) grant 278/18 to ABZ and grant 372/17 to DM. L.M. was supported by the Ministry of Science and Technology, Yitzhak Navon Ph.D. fellowship, and Kreitman Biotech scholarship. D.B. and T.C. were supported by the Kreitman Negev scholarships.

Availability of data and materials

All data generated or analyzed during this study are included in this published article and its supplementary information files. Individual data values are included in Additional file 2. The sequencing datasets analyzed in the current study are available in the NCBI Sequence Read Archive repository accession number SRP018046 [30], <http://www.ncbi.nlm.nih.gov/sra>.

Declarations

Ethics approval and consent to participate

Not applicable.

Consent for publication

Not applicable.

Competing interests

The authors declare that they have no competing interests.

Author details

¹Department of Life Sciences, Ben-Gurion University of the Negev, Beer Sheva, Israel. ²Department of Microbiology, Immunology and Genetics, Ben-Gurion University of the Negev, Beer Sheva, Israel. ³Department of Neurology, Department of Laboratory Medicine and Pathology, Mayo Clinic, Rochester, MN, USA. ⁴Dr. John T. Macdonald Foundation Department of Human Genetics and Hussman Institute for Human Genomics, Miller School of Medicine, University of Miami, Miami, FL, USA. ⁵Institute of Neurology, Schneider Children's Medical Center of Israel, Tel-Aviv University, Petach Tikva, Israel.

Received: 22 June 2021 Accepted: 28 January 2022
Published online: 09 February 2022

References

- Schon EA, Gilkerson RW. Functional complementation of mitochondrial DNAs: mobilizing mitochondrial genetics against dysfunction. *Biochimica et Biophysica Acta (BBA)-General Subjects*. 2010;1800(3):245–9.
- Avital G, Buchshtav M, Zhidkov I, Tuval Feder J, Dadon S, Rubin E, et al. Mitochondrial DNA heteroplasmy in diabetes and normal adults: role of acquired and inherited mutational patterns in twins. *Hum Mol Genet*. 2012;21(19):4214–24.
- Goto H, Dickins B, Afgan E, Paul IM, Taylor J, Makova KD, et al. Dynamics of mitochondrial heteroplasmy in three families investigated via a repeatable re-sequencing study. *Genome Biol*. 2011;12(6):R59.
- Wei W, Tuna S, Keogh MJ, Smith KR, Aitman TJ, Beales PL, et al. Germline selection shapes human mitochondrial DNA diversity. *Science*. 2019;364(6442).
- Zaidi AA, Wilton PR, Su MS, Paul IM, Arbeithuber B, Anthony K, et al. Bottleneck and selection in the germline and maternal age influence transmission of mitochondrial DNA in human pedigrees. *Proc Natl Acad Sci U S A*. 2019;116(50):25172–8.
- Sharpley MS, Marciniak C, Eckel-Mahan K, McManus M, Crimi M, Waymire K, et al. Heteroplasmy of mouse mtDNA is genetically unstable and results in altered behavior and cognition. *Cell*. 2012;151(2):333–43.
- Latorre-Pellicer A, Lechuga-Vieco AV, Johnston IG, Hamalainen RH, Pellico J, Justo-Mendez R, et al. Regulation of mother-to-offspring transmission of mtDNA heteroplasmy. *Cell Metab*. 2019;30(6):1120–1130 e1125.
- Hahn A, Zuryn S. The cellular mitochondrial genome landscape in disease. *Trends Cell Biol*. 2019;29(3):227–40.
- Craven L, Alston CL, Taylor RW, Turnbull DM. Recent Advances in Mitochondrial Disease. *Annu Rev Genomics Hum Genet*. 2017;18:257–75.
- Floros VI, Pyle A, Dietmann S, Wei W, Tang WCW, Irie N, et al. Segregation of mitochondrial DNA heteroplasmy through a developmental genetic bottleneck in human embryos. *Nat Cell Biol*. 2018;20(2):144–51.
- Burgstaller JP, Johnston IG, Jones NS, Albrechtova J, Kolbe T, Vogl C, et al. MtDNA segregation in heteroplasmic tissues is common in vivo and modulated by haplotype differences and developmental stage. *Cell Rep*. 2014;7(6):2031–41.
- Jeedigunta SP, Minenkova AV, Palozzi JM, Hurd TR. Avoiding extinction: recent advances in understanding mechanisms of mitochondrial DNA purifying selection in the germline. *Annu Rev Genomics Hum Genet*. 2021;22:55–80.
- Suen DF, Narendra DP, Tanaka A, Manfredi G, Youle RJ. Parkin overexpression selects against a deleterious mtDNA mutation in heteroplasmic cybrid cells. *Proc Natl Acad Sci U S A*. 2010;107(26):11835–40.
- Valenci I, Yonai L, Bar-Yaacov D, Mishmar D, Ben-Zvi A. Parkin modulates heteroplasmy of truncated mtDNA in *Caenorhabditis elegans*. *Mitochondrion*. 2015;20:64–70.
- Lin Y-F, Schulz AM, Pellegrino MW, Lu Y, Shaham S, Haynes CM. Maintenance and propagation of a deleterious mitochondrial genome by the mitochondrial unfolded protein response. *Nature*. 2016;533(7603):416.
- Gitschlag BL, Kirby CS, Samuels DC, Gangula RD, Mallal SA, Patel MR. Homeostatic responses regulate selfish mitochondrial genome dynamics in *C. elegans*. *Cell Metab*. 2016;24(1):91–103.
- Ahier A, Dai CY, Kirmes I, Cummins N, Hung GCC, Gotz J, et al. PINK1 and parkin shape the organism-wide distribution of a deleterious mitochondrial genome. *Cell Rep*. 2021;35(9):109203.
- Mao K, Wang K, Liu X, Klionsky DJ. The scaffold protein Atg11 recruits fission machinery to drive selective mitochondria degradation by autophagy. *Dev Cell*. 2013;26(1):9–18.
- Twig G, Elorza A, Molina AJA, Mohamed H, Wikstrom JD, Walzer G, et al. Fission and selective fusion govern mitochondrial segregation and elimination by autophagy. *Embo J*. 2008;27(2):433–46.
- Malena A, Loro E, Di Re M, Holt IJ, Vergani L. Inhibition of mitochondrial fission favours mutant over wild-type mitochondrial DNA. *Hum Mol Genet*. 2009;18(18):3407–16.
- Kandul NP, Zhang T, Hay BA, Guo M. Selective removal of deletion-bearing mitochondrial DNA in heteroplasmic *Drosophila*. *Nat Commun*. 2016;7:13100.
- Lieber T, Jeedigunta SP, Palozzi JM, Lehmann R, Hurd TR. Mitochondrial fragmentation drives selective removal of deleterious mtDNA in the germline. *Nature*. 2019;570(7761):380–4.
- Gilkerson RW, Schon EA, Hernandez E, Davidson MM. Mitochondrial nucleoids maintain genetic autonomy but allow for functional complementation. *J Cell Biol*. 2008;181(7):1117–28.
- Busch KB, Kowald A, Spelbrink JN. Quality matters: how does mitochondrial network dynamics and quality control impact on mtDNA integrity? *Philos Trans R Soc Lond B Biol Sci*. 2014;369(1646):20130442.
- Rebolledo-Jaramillo B, Su MS-W, Stoler N, McElhroe JA, Dickins B, Blankenberg D, et al. Maternal age effect and severe germ-line bottleneck in the inheritance of human mitochondrial DNA. *Proc Natl Acad Sci*. 2014;111(43):15474–9.
- Ye K, Lu J, Ma F, Keinan A, Gu Z. Extensive pathogenicity of mitochondrial heteroplasmy in healthy human individuals. *Proc Natl Acad Sci*. 2014;111(29):10654–9.
- Tsang WY, Lemire BD. Stable heteroplasmy but differential inheritance of a large mitochondrial DNA deletion in nematodes. *Biochem Cell Biol*. 2002;80(5):645–54.
- Liau W-S, Gonzalez-Serricchio AS, Deshommes C, Chin K, CW LM. A persistent mitochondrial deletion reduces fitness and sperm performance in heteroplasmic populations of *C. elegans*. *BMC Genet*. 2007;8(1):8.
- Thompson O, Edgley M, Strasbourger P, Flibotte S, Ewing B, Adair R, et al. The million mutation project: a new approach to genetics in *Caenorhabditis elegans*. *Genome Res*. 2013;23:1749–62.
- The Million Mutation Project – *C. elegans* Mutation Resource. In: NCBI Sequence Read Archive repository; 2012. <https://tracencbinlmnihgov/Traces/sra/?study=SRP018046>.
- Bratic I, Hench J, Henriksson J, Antebi A, Burglin TR, Trifunovic A. Mitochondrial DNA level, but not active replicase, is essential for *Caenorhabditis elegans* development. *Nucleic Acids Res*. 2009;37(6):1817–28.
- Ahier A, Dai CY, Tweedie A, Bezawork-Geleta A, Kirmes I, Zuryn S. Affinity purification of cell-specific mitochondria from whole animals resolves patterns of genetic mosaicism. *Nat Cell Biol*. 2018;20(3):352–60.
- Tanaka A, Cleland MM, Xu S, Narendra DP, Suen DF, Karbowski M, et al. Proteasome and p97 mediate mitophagy and degradation of mitofusins induced by Parkin. *J Cell Biol*. 2010;191(7):1367–80.
- Basso V, Marchesan E, Peggion C, Chakraborty J, von Stockum S, Giacomello M, et al. Regulation of ER-mitochondria contacts by Parkin via Mfn2. *Pharmacol Res*. 2018;138:43–56.
- Yasuda K, Hartman PS, Ishii T, Suda H, Akatsuka A, Shoyama T, et al. Interrelationships between mitochondrial fusion, energy metabolism and oxidative stress during development in *Caenorhabditis elegans*. *Biochem Biophys Res Commun*. 2011;404(3):751–5.
- Byrne JJ, Soh MS, Chandhok G, Vijayaraghavan T, Teoh JS, Crawford S, et al. Disruption of mitochondrial dynamics affects behaviour and lifespan in *Caenorhabditis elegans*. *Cell Mol Life Sci*. 2019;76(10):1967–85.
- Luz AL, Rooney JP, Kubik LL, Gonzalez CP, Song DH, Meyer JN. Mitochondrial morphology and fundamental parameters of the mitochondrial respiratory chain are altered in *caenorhabditis elegans* strains deficient in mitochondrial dynamics and homeostasis processes. *Plos One*. 2015;10(6):e0130940.
- Champilas N, Tavernarakis N. Mitochondrial maturation drives germline stem cell differentiation in *Caenorhabditis elegans*. *Cell Death Differ*. 2020;27(2):601–17.
- Raiders SA, Eastwood MD, Bacher M, Priess JR. Binucleate germ cells in *Caenorhabditis elegans* are removed by physiological apoptosis. *Plos Genet*. 2018;14(7):e1007417.
- Bohnert KA, Kenyon C. A lysosomal switch triggers proteostasis renewal in the immortal *C. elegans* germ lineage. *Nature*. 2017;551(7682):629–33.
- Tang Y, Manfredi G, Hirano M, Schon EA. Maintenance of human rearranged mitochondrial DNAs in long-term cultured transmitochondrial cell lines. *Mol Biol Cell*. 2000;11(7):2349–58.
- Meshnik L, Bar-Yaacov D, Kasztan D, Neiger T, Cohen T, Kishner M, et al. Mutant *C. elegans* mitofusin leads to selective removal of mtDNA heteroplasmic deletions at different rates across generations. *bioRxiv*. 2020. <https://doi.org/10.1101/610758>.
- de Brito OM, Scorrano L. Mitofusin 2 tethers endoplasmic reticulum to mitochondria. *Nature*. 2008;456(7222):605–10.

44. Friedman JR, Lackner LL, West M, DiBenedetto JR, Nunnari J, Voeltz GK. ER tubules mark sites of mitochondrial division. *Science*. 2011;334(6054):358–62.
45. Gautier CA, Erpapazoglou Z, Mouton-Liger F, Muriel MP, Cormier F, Bigou S, et al. The endoplasmic reticulum-mitochondria interface is perturbed in PARK2 knockout mice and patients with PARK2 mutations. *Hum Mol Genet*. 2016;25(14):2972–84.
46. Larrea D, Pera M, Gonnelli A, Quintana-Cabrera R, Akman HO, Guardia-Laguarta C, et al. MFN2 mutations in Charcot-Marie-Tooth disease alter mitochondria-associated ER membrane function but do not impair bioenergetics. *Hum Mol Genet*. 2019;28(11):1782–800.
47. Sharma A, Smith HJ, Yao P, Mair WB. Causal roles of mitochondrial dynamics in longevity and healthy aging. *Embo Rep*. 2019;20(12).
48. Shai N, Shemesh N, Ben-Zvi A. Remodeling of proteostasis upon transition to adulthood is linked to reproduction onset. *Curr Genomics*. 2014;15(2):122–9.
49. Levin L, Mishmar D. A genetic view of the mitochondrial role in ageing: killing us softly. *Adv Exp Med Biol*. 2015;847:89–106.
50. Livak KJ, Schmittgen TD. Analysis of relative gene expression data using real-time quantitative PCR and the 2⁻(Delta Delta C(T)) Method. *Methods*. 2001;25(4):402–8.

Publisher's Note

Springer Nature remains neutral with regard to jurisdictional claims in published maps and institutional affiliations.

Ready to submit your research? Choose BMC and benefit from:

- fast, convenient online submission
- thorough peer review by experienced researchers in your field
- rapid publication on acceptance
- support for research data, including large and complex data types
- gold Open Access which fosters wider collaboration and increased citations
- maximum visibility for your research: over 100M website views per year

At BMC, research is always in progress.

Learn more biomedcentral.com/submissions

